Synthesis of electron transmission in nanoscale semiconductor devices

Petra Schmidt and Stephan Haas
Department of Physics and Astronomy, University of Southern California, 3620 South McClintock Avenue, SSC 211A, Los Angeles, California 90089-0484

A. F. J. Levi
Department of Physics and Astronomy, University of Southern California, 3620 South McClintock Avenue, SSC 211A, Los Angeles, California 90089-0484 and Department of Electrical Engineering, University of Southern California, 3620 South Vermont Avenue, KAP 132, Los Angeles, California 90089-2533

(Received 25 July 2005; accepted 3 November 2005; published online 3 January 2006)

Adaptive design may be used to synthesize a conduction band potential profile to obtain desired nonequilibrium electron transmission-voltage characteristics. Our methodology is illustrated by designing a two-terminal linear element in which electron motion is limited by quantum mechanical transmission through a potential profile. © *2006 American Institute of Physics*.
[DOI: 10.1063/1.2159102]

The scaling of classical semiconductor devices such as the transistor[1] will eventually be limited by quantum effects. In this situation typical semiconductor device dimensions are a few nanometers. The resulting large electric fields give rise to tunneling and nonequilibrium behavior that include ballistic electron transport. While nonlinear devices such as transistors can be created that exploit these transport phenomena,[2] it is unknown if devices with controlled linear and other power law response can be scaled into the quantum regime. Such devices are required because, for example, a linear resistor is a critical element for analog and low power circuit design. In this letter, we show that it is, in fact, possible to design such devices and, contrary to initial expectations, linear response is not excluded by the exponential dependencies normally associated with electron tunneling in semiconductors.

In stark contrast to diffusive electron transport that gives rise to Ohm's law in classical devices,[3] nonequilibrium electron transmission through nanoscale semiconductor devices can be ballistic and the resulting behavior is non-Ohmic. Let us consider electron transport through a rectangular barrier of energy $V_0=0.3$ eV and width $L=4$ nm, as shown in Fig. 1. The barrier is sandwiched between n-type electrodes with carrier concentration $n=10^{18}$ cm^{-3}. Applying a bias voltage, V_{bias}, results in a depletion region on the right side and an accumulation region on the left side of the barrier. The form of the conduction band profile $V(x)$ in these regions is calculated by solving the Poisson equation.[4] Electron motion is in the x direction, normal to the barrier plane and there is no confinement in the y and z directions, thereby avoiding possible detrimental consequences of quantized conductance.[5] A numerical solution to the Schrödinger equation is obtained piecewise by discretizing the potential profile into 4000 steps, matching boundary conditions at each interface, and implementing the propagation matrix method.[6] An electron of energy $E=26$ meV incident from the left is partially reflected and partially transmitted, as determined by the wave function boundary conditions $\psi_j=\psi_{j+1}$ and $\partial\psi_j/\partial x=\partial\psi_{j+1}/\partial x$ at each interface. Here ψ_j is a solution of Schrödinger's equation in region j with wave vector $k_j=\sqrt{2m(E-eV_j)}/\hbar$, where V_j is the local potential in the conduction band and m is the effective electron mass.

Exponential increase in electron transmission with bias voltage is a generic feature of the simplest barrier profiles. Potential wells, on the other hand, are known to produce bound state resonances, leading to sharp transmission peaks. Hence, design of structures with linear and other power-law transmission-voltage characteristics likely involves broken-symmetry potential barrier profiles. As an initial challenge in our exploration of this possibility we use an adaptive quantum design approach[7] to find a potential profile with a transmission function $T(V_{\mathrm{bias}})$ that increases *linearly* with bias voltage in the window $0\ \mathrm{V}<V_{\mathrm{bias}}<0.25$ V.

We define the conduction band potential energy profile on a grid with $\Delta x=2$ nm ($\sim$8 monolayers in GaAs) spatial increments and $\Delta V=0.01$ eV energy increments. The numerical search for optimal broken-symmetry barrier profile is constrained to take into account physical as well as computational limitations. Physically, varying the composition of an $\mathrm{Al}_x\mathrm{Ga}_{1-x}\mathrm{As}$ alloy controls the conduction band potential profile. Fabrication inaccuracies of 1–2 monolayers may occur in the epitaxial growth processes, and hence, the targeted transmission functionality needs to remain stable against such variations. Moreover, the Al concentration can only be controlled to within a few percent. Computationally, the complexity of the physical model and the dimensionality of the search space needs to be constrained in order to match the available computer hardware capabilities.[8] For this reason, the physical model we use does not solve the Schrödinger equation and Poisson equation self-consistently and to keep the search space finite, we focus on nanoscale barrier structures of total width $L=10$ nm with a maximum on-site potential of 0.3 eV measured from the GaAs conduction band minimum.

Figure 2 shows solutions from exhaustive numerical searches for conduction band profiles that give linear and square-law $T(V_{\mathrm{bias}})$ characteristics. For the discrete grid discussed above, the size of the search space is $30^5\approx 2.4\times 10^7$. The resulting broken-symmetry barrier solutions are sequences of rectangular steps. For the case of a linear target function [Figs. 2(a) and 2(b)], the quadratic deviation of the obtained solution from the target is $\chi^2=5.1\times 10^{-7}$. When we restrict our search to monotonically decreasing potentials the reduced size of the search space

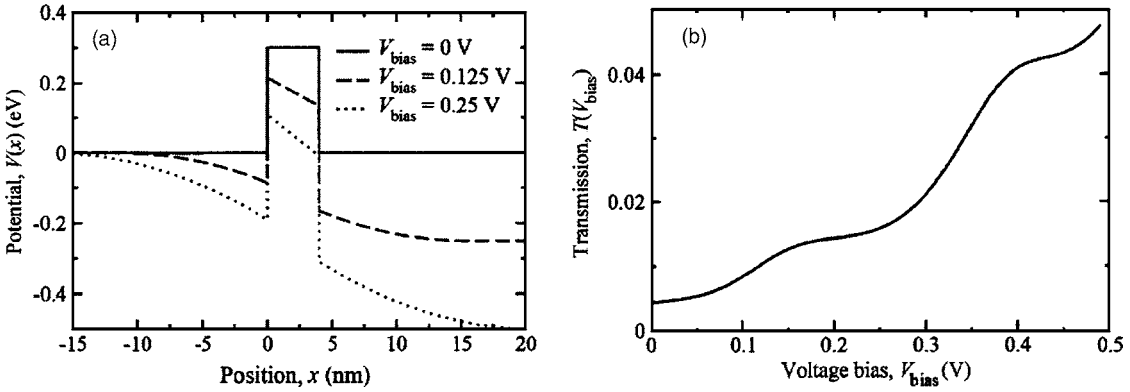

FIG. 1. A rectangular potential barrier of energy V_0=0.3 eV and width L=4 nm gives rise to rapid increase in electron transmission with increasing voltage bias, V_{bias} and resonances. Effective electron mass is $m=0.07m_0$, where m_0 is the bare electron mass. (a) Conduction band profile of the rectangular potential barrier for the indicated values of V_{bias}. (b) Transmission probability as a function of V_{bias} for an electron of energy E=26 meV incident from the left.

allows us to consider a finer grid in space with Δx=1 nm ($\sim$4 monolayers in GaAs). The size of the search space is now $40!/(10!30!)\approx 8.5\times 10^8$. In this case the quadratic deviation of the obtained solution from the linear target is $\chi^2=4.5\times 10^{-6}$. In Fig. 2(c) the solution of an exhaustive search for a barrier profile with a quadratic transmission-voltage characteristic is shown. Here, the square deviation between solution and target is $\chi^2=5.6\times 10^{-8}$.

Our results show it is possible to construct semiconductor nanoscale structures with desired linear and power-law electron transmission-voltage characteristics. In such devices elastic scattering limits ballistic electron current flow and dissipative relaxation processes occur in the electrodes. However, there is a hierarchy of target functionalities, some are more accessible than others using the available building blocks. For example a square-root target response poses a much more challenging problem and the best solution identified by the exhaustive numerical search for this functionality only has $\chi^2=6.6\times 10^{-5}$.

We find it remarkable that a linear response in a ballistic nanostructure may be achieved by solely utilizing the physical ingredient of elastic scattering and tunneling at potential steps. To better understand the physics enabling power-law transmission as a function of V_{bias} we consider the progressive evolution of solutions for the linear target from a simple square barrier to the multibarrier profile of Fig. 2(a). As illustrated in Figs. 3(a) and 3(b), the dominant transmission features of the simple square well, i.e., the exponential behavior and resonances, are altered by the addition of steps in the potential barrier profile. It is observed that the superposition of broad resonances due to the presence of different potential steps helps linearize the transmission-voltage curve.

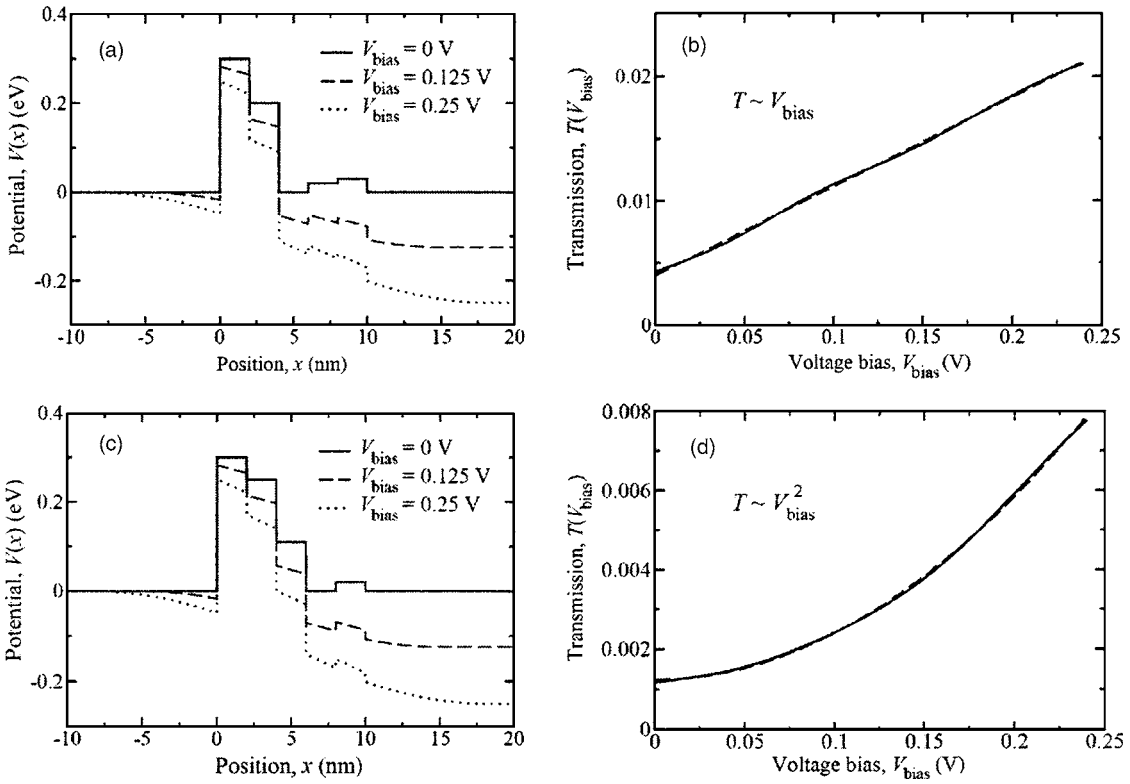

FIG. 2. (a) and (c) are solutions from exhaustive numerical searches for conduction band profiles $V(x)$ that yield linear and square dependences of electron transmission as a function of bias voltage, V_{bias}. $V(x)$ is constrained to a region that is 10 nm wide and the maximum local potential is 0.3 eV. The resulting $T(V_{bias})$ for an electron of energy E=26 meV incident from the left are shown as solid line in (b) and (d). Broken line is target response.

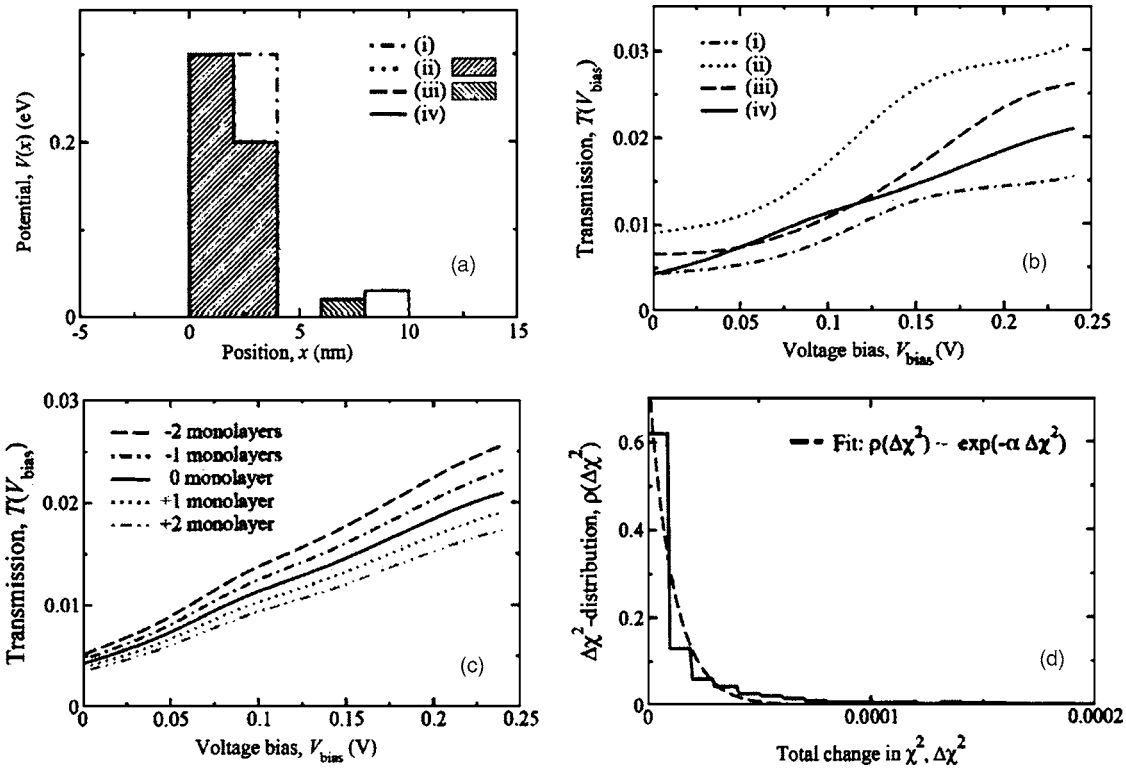

FIG. 3. (a) Evolution from a single potential barrier to an array of barriers. (b) $T(V_{\text{bias}})$ for the potentials in (a). The superposition of broad resonances enables a linear transmission-voltage response. (i) single rectangular barrier of 4 nm, (ii) 4 nm wide barrier with a step, (iii) same as (ii) plus 1 nm wide small barrier, (iv) optimized potential profile. (c) Changes of 1–2 monolayers at the initial highest barrier mainly alters the slope of the transmission curve, i.e., the resistance. (d) Randomly selected 0, ±1, and ±2 monolayer changes at all interfaces only lead to small deviations in χ^2. The characteristic variation in χ^2 is $1/\alpha = 1.1 \times 10^{-5}$.

It is also this superposition of broad scattering resonances which renders the solution stable against small perturbations.

Robustness of a solution to monolayer changes at each interface in the barrier array may be explored using sensitivity analysis. Results presented in Fig. 3(c) show that the slope of $T(V_{\text{bias}})$ is determined by the initial highest barrier energy, whereas its smoothness is governed by the low barrier energy tail of the array that controls the fast spatial modulations of the electron wave in the structure. Therefore, depending on the position of the deviations from the original structure, different components of the response function are affected. We have also explored the effect of smoothing the edges in the conduction band profile. Error function rounding of interfaces on the scale of 2 monolayers changes the linear transmission-voltage response of Fig. 2(b) only slightly, yielding a quadratic deviation of $\chi^2 = 5.7 \times 10^{-7}$.

In Fig. 3(d) results are shown from a study of randomly selected 0, ±1, and ±2 monolayer changes at all interfaces in the barrier structure. The effect is relatively small, yielding an average change of $1/\alpha \approx 10^{-5}$ in χ^2, where α is the parameter of the exponential fit in Fig. 3(d). Moreover, the sensitivity of χ^2 to changes in the potential energy due to random variations on the order of 1% in the Al concentration of $Al_xGa_{1-x}As$ is found to be similar. Hence, the transmission characteristics enabled by the conduction band potential profile discussed in this letter are stable against small random variations.

In conclusion, we have demonstrated that adaptive design can be applied to the synthesis of nanoscale devices with power-law transmission-voltage characteristics. Using a constrained exhaustive numerical search, broken-symmetry conduction band profiles of semiconductor heterostructures have been identified which enable desired quantum transport functionality. This custom-designed superposition of broad scattering resonances due to the presence of an optimal potential makes it possible to "recreate" Ohm's law within a window of bias voltages in a system that is dominated by ballistic electron transport. In particular, one can synthesize a nanoscale two-terminal linear resistive element that is robust against monolayer perturbations.

This work is supported by DARPA and ONR.

[1] G. E. Moore, Electronics **38**, 114 (1965); also reprinted in Proc. IEEE **86**, 82 (1998).
[2] For example, T. H. Chiu and A. F. J. Levi, Appl. Phys. Lett. **55**, 1891 (1989).
[3] For example, W. A. Harrison, Phys. Rev. **123**, 85 (1961).
[4] For example, S. Wang, *Fundamentals of Semiconductor Theory and Device Physics* (Prentice Hall, Englewood Cliffs, N.J., 1989).
[5] R. Landauer, IBM J. Res. Dev. **1**, 223 (1957); R. Landauer, Philos. Mag. **21**, 863 (1970); M. Buttiker, Y. Imry, R. Landauer, and S. Pinhas, Phys. Rev. B **31**, 6207 (1985); M. Buttiker, J. Phys.: Condens. Matter **5**, 9361 (1993); T. Christen and M. Buttiker, Europhys. Lett. **35**, 523 (1996); D. Sanchez and M. Buttiker, Phys. Rev. Lett. **93**, 106802 (2004).
[6] For example, G. Bastard, Phys. Rev. B **24**, 5693 (1981).
[7] J. Thalken, W. Li, S. Haas, and A. F. J. Levi, Appl. Phys. Lett. **85**, 121 (2004).
[8] In this case we use the University of Southern California High Performance Computer Cluster (HPCC) parallel computer with 1436 nodes (2872 CPUs).